Physical Properties, UV Stability, Biodegradability, and DFT Study of Chicken Feather Fiber Based Composites Crosslinked with Rosin Derivative

Gitashree Gogoi
Tezpur University
Arpita Joarder
Tezpur University
Pritam Bardhan
Tezpur University
Dikshita Dowerah
Tezpur University
Manabendra Mandal
Tezpur University
Ramesh C. Deka
Tezpur University
Tarun K. Maji (tkm@tezu.ernet.in)
Tezpur University

Research Article

Keywords: Chicken Feather, Rosin acid derivative, Biocomposites, UV resistance, Mechanical properties, Thermal properties

Posted Date: June 14th, 2022

DOI: https://doi.org/10.21203/rs.3.rs-1736985/v1

Abstract

Composites due to its advantageous properties for different construction purposes and outdoor applications have gained significant popularity in recent years. Biocomposites had gained importance, mainly due to their eco-friendly and processibility profile. Chicken Feather Fiber (CFF) composite based on modified epoxidized soybean oil (ESO) and natural crosslinker was prepared via compression molding technique. Methacrylic anhydride epoxidized soybean oil (MAESO) as resin, chicken feather fiber flour as a reinforcing agent, and rosin derivative as crosslinker was used to develop the final bio-composite. The fiber/resin ratio was maintained at 30:70 and the percentage of rosin derivative was varied from 0–40 (wt%). The resulting bio-composites were characterized by Fourier transformed infrared (FT-IR) spectroscopy also supported by Density Functional Theory (DFT) calculations. Thermogravimetric analysis (TGA) was done to observe the thermal stability of the bio-composites. Scanning Electron Microscope (SEM) showed the morphology of the biocomposites. Hardness Test, limiting oxygen index (LOI), chemical resistance, water absorption behavior was checked for the prepared bio-composites. An enhanced UV resistance was observed for the composites loaded with rosin derivative as supported by lower weight loss, carbonyl index, and SEM analysis. Composite based on 30 wt% of TM revealed highest enhancement in all the properties.

1. Introduction

In recent years, much attention has centered on the use of composite materials due to its numerous advantages. With increasing environmental concerns and depleting petroleum reserves, bio-composites are gaining more attention as they are environmentally sustainable [1]. Natural fiber reinforced polymer composites are achieving demand mainly due to their light weight, low cost, and eco-friendly behavior [2]. Other advantages include good specific properties, easy availability, good mechanical strength, corrosion resistance, chemical resistance, and biodegradability [3]. Due to such qualities, natural fiber reinforced composites have found huge applications in the field of engineering.

Natural fibers like chicken feather fibers display satisfactory mechanical properties, possess lowest density, are environment friendly, have excellent acoustic and high thermal insulation properties [4, 5]. All these advantages have triggered researchers to investigate more on chicken feather reinforced composites. Also, the disposal of chicken feathers is a major environmental issue as they produce greenhouse gases [6–8]. Thus to overcome this issue chicken feathers can add value as reinforcing fibers in fabricating composites. Chicken feathers are mostly composed of keratin proteins (approx. 90%) and amino acids [9]. The matrix used in bio-composites may be synthetic or natural resins. In fiber reinforced polymer composites, the mechanical performance is provided by the fiber-matrix interface, which helps in transferring stress within the composite [10]. Thermosetting resins are the best candidates for the production of fiber reinforced polymer composites, because of their good chemical resistance, thermal resistance, and mechanical properties. The thermosetting resins obtained from vegetable/plant oils such as soybean, linseed, etc. are ecofriendly, readily available, and can be used as a polymer matrix for preparing biocomposites.

Soybean oil is one of the low-cost and most easily available vegetable oils in the world [11]. The main component present in the oil is the triglyceride part. The triglyceride atoms have three fatty acids connected by glycerol in the center [12, 13]. The soybean oil itself cannot provide the resin with desired stiffness or structural strength. Thus, modification of some of the reactive sites of soybean oil such as epoxidation of the double bond of the soybean oil to produce epoxidized soybean oil (ESO) is done [14]. The epoxy groups in the ESO can further be modified. Acrylate or methacrylate functions are introduced in the polymer for polymerization or copolymerization of the double bonds to form a network or grafted copolymers [14]. Due to the long soft aliphatic chain of the fatty acid, the resulted resins usually display unsatisfied mechanical and thermal properties [15]. To improve such properties, petroleum-based rigid comonomers such as styrene or divinylbenzene (DVB) are employed. However, such components are extremely hazardous to the environment and they are volatile organic compounds [16]. Also, the use of such components reduces the bio-based content of the final materials. Thus, it is important to search for alternatives to replace these petroleum-based components with bio-based monomers which can improve the properties as well as decrease the unwanted effects on the environment [17].

In recent times, rosin acid has been of notice for the synthesis of new polymeric materials because it is abundant, cheap, biodegradable, biocompatible, and has a special structure that can be chemically modified [18]. Rosin acid is the main component (about 90%) of the crude rosin obtained from the exudation of pines and conifers [19]. Rosin acid is mainly composed of abietic acid, levopimaric acid, and pimaric acid [20]. It is a mixture of monocarboxylic acids having a hydrophenanthrene ring structure. The phenanthrene ring structure of rosin acids is a rigid entity and has the potential to make the rosin acid derivatives a major replacement for traditional petroleum-based rigid monomers [21, 22].

Taking into consideration the benefits of biobased composites and the growing desire for greener products, the present study aims to develop a biobased composite comprising chicken feathers as a reinforcing agent, methacrylic anhydride epoxidized soybean oil (MAESO) as the matrix and Triallyl maleopimarate (TM) as crosslinker. The materials employed in this report are based on natural sources and thus the composites are anticipated to be biodegradable. There is very less record in this regard. Hence, there is ample scope for extensive research in this area. The resulting bio-composites are loaded with different percentages of TM, which serves as the crosslinker keeping the amount of chicken feather fiber flour constant, the percentage of TM was varied and the various properties of the composites have been analyzed. The reaction scheme and structures of rosin acid and TM are presented in Fig. 1.

2. Experimental

2.1 Materials

Chicken feather fibers were bought from a poulterer in Tezpur (India). Rosin acid was obtained from Alfa aesar (USA). Epoxidized soybean oil (ESO) was received from Agrawal Organics (India). Acetic acid, Sodium hydroxide, Hydrochloric acid, potassium carbonate were purchased from Rankem (India). N-methylimidazole and Methacrylic acid were obtained from Merck (India). Tert-butyl peroxybenzoate,

Methacrylic anhydride, Cobalt (II) ethylhexanoate were procured from Sigma Aldrich, (USA). Maleic anhydride (extrapure AR, 99%) was obtained from SRL Chemicals, India. Hydroquinone was bought from G.S. Chemical Testing Lab & Allied Industries, India. Allyl bromide (for synthesis) was purchased from Loba Chemie, (India). The other reagents received were used directly in this study.

2.2 Synthesis of Resin

The resin was synthesized as per the procedure of Gogoi et al. [23].

2.3 Synthesis of maleopimaric anhydride (MA)

In a three-necked round bottom flask, upon a magnetic stirrer, reflux condenser, and a magnetic needle, 10g of rosin acid was heated for 3h at 180°C, under an inert atmosphere and then allowed to cool down at 120°C. 30mL of acetic acid was added to it. In the mixture, 2.35g of maleic anhydride, 0.46g of p-toluene sulphonic acid were included. The reaction was then refluxed for 12h at 120°C and after cooling a solid (yellow color) was obtained. Recrystallization of the product was carried out with acetic acid to obtain white color maleopimaric anhydride (MA)[18].

2.4 Synthesis of triallyl maleopimarate (TM)

In a round bottom flask, 20g of MA, 20g of NaOH, and 125 mL of distilled water were stirred at 120°C and refluxed for 12h. Then, 225mL of aqueous hydrochloric acid solution (2mol/L) was added dropwise and then adjusted to neutral. The precipitate formed was collected and washed several times with deionized water. This intermediate product (MPAc) was then dried and kept ready for further reaction.

In a round bottom flask, 20.9g of MPAc, 26.15g of potassium carbonate, and 60mL of acetone were added under mechanical stirring. A solution of 30.25g of allyl bromide dissolved in 7.5mL of acetone was then added dropwise and refluxed at 70°C for 12h. The organic phase was extracted, washed with deionized water and in a rotary evaporator at 80°C the solvents were removed. Finally, a dark yellow color product named TM was obtained.

2.5 Pre-treatment of Chicken Feathers

The Chicken feather was washed thoroughly with water and soap (1%) to draw out the dirts. To enhance surface roughness and discard fats, it was treated with NaOH (1%) solution followed by sun drying for few days. The feathers were then grinded, sieved (70 mesh) to powder or flour form for experiments.

2.6 Preparation of biocomposites

To develop the composites, triallyl maleopimarate (TM) was added to the MAESO resin in a beaker as per the formulation presented in Table 1 and stirred till proper mixing. Afterward, Cobalt (II)- 2 ethylhexanoate (1% promoter) was added to the resin mixture. Subsequently to this, tert-butylperoxybenzoate (TBP) (2% catalyst) was added and stirred. Chicken feather fibers flour was added to that resin mixture and mixed properly for several minutes. The resin/fiber mixture was then transferred to a tray and kept ready for the preparation of the composite. The sheets were prepared by employing a manual compression molding

press (S.C.Dey Co. Kolkata). The resin/fiber (70:30) mixture was placed in between the mold plates and compression-molded at 140°C for 30 mins. The mold was then allowed to cool to get the final composite sheets. A probable reaction mechanism for the resin (MAESO), TM, and CF is presented in Fig. 2. The cysteine part of chicken feather was taken into account for the elucidation of the reaction mechanism.

Table 1
Composition used for the preparation of composites

Sample name	MAESO (wt%)	TM (wt%)	Promoter (wt%)	TBP (wt%)	CF (wt%)
MAESO/CF/TM0	70	0	1	2	30
MAESO/CF/TM20	50	20	1	2	30
MAESO/CF/TM30	40	30	1	2	30
MAESO/CF/TM40	30	40	1	2	30

2.7 Culture media preparation

Mineral salt medium (MSM) with the given composition was prepared for bacterial growth: Na_2HPO_4, 2 g; $(NH_4)_2SO_4$, 2 g; KH_2PO_4, 4.75 g; $MgSO_4$, 1.2 g; H_3BO_3, 10 mg; MoO_3, 10 mg; $ZnSO_4$,70 mg;$CaCl_2$, 0.5 mg, $CuSO_4.7H_2O$, 100 mg; $MnSO_4$, 100 mg; $FeSO_4$, 1 mg; Distilled water,1000 mL. 500 mL of this medium was transferred in a 1L Erlenmeyer flask and sterilized by autoclaving at 121°C, 15 psi pressure for 20 min. The sterile medium was then allowed to cool down. The samples were exposed to UV light for 10 min each (on both sides) and added into the medium under sterile condition inside a laminar airflow hood. Media containing samples without bacterial culture was taken as negative control.

2.8 Inoculum preparation

The inoculums were prepared by using a co-culture of bacteria (18 h old culture of Bacillus cereus MTCC 430 and Pseudomonas aeruginosa MTCC 3541) grown in Luria Bertani broth medium (HiMedia) and was centrifuged at 10000 rev min^{-1} for 10 min. The pellet was cleansed with 0.9% NaCl solution and resuspended in a 1 mL mineral salt medium. In a centrifuge tube, 20 mL of all sterilized MSM was inoculated with 0.5 mL of 0.6 $O.D_{600\ nm}$ bacterial cultures. The test tubes were then incubated at 37°C, 140 rev min^{-1}. Absorbance was recorded at 600 nm after every 7 days to monitor bacterial growth.

3. Characterizations

3.1 Fourier Transform Infrared Spectroscopy (FT-IR)

FT-IR study was performed in an FT-IR spectrophotometer (Perkin Elmer, MIR-FIR, USA) using the KBr pellet technique in 4000–400 cm^{-1} wavelength range.

3.2 Computational details

Stability of the probable structure for the composites (MAESO/TM/CF, Fig. 2.) has been supported by the outcome of Density Functional Theory (DFT) calculations. Structures of the reactants Rosin acid, MAESO, TM, CF were modeled based on experimentally available crystal structure information using the molecular building and visualization tool Gauss View [24]. Geometry optimization has been done on all the titled molecules to achieve the lowest energy structures using the Gaussian09 software program [24]. Energy minimization along with frequency calculations were done employing the B3LYP functional with triple-ζ split valence diffused basis set 6-311G(d,p) for all atoms, without imposing any symmetry constraints [25–27]. Frequency calculations were done to distinguish between minima (NIMAG = 0) and first-order maxima (NIMAG = 1). Water was added as the solvent implicitly using the conductor-like polarizable continuum solvation model (CPCM) [28].

3.3 Thermogravimetric analysis (TGA)

An analyzer (TGA-50, Shimadzu, Singapore) was used for thermal stability. A heating rate of 10°C min^{-1} from 25–600°C was kept under an inert atmosphere with a flow rate of 30mL min^{-1}.

3.4 Limiting Oxygen Index (LOI)

A flammability tester (S.C. Dey Co., India) was employed for the test by using ASTM-D 2863. LOI values were decided by considering the lowest ratio of oxygen and nitrogen where the composites burned for 30 sec.

LOI = Volume of O_2 / Volume of ($O_2 + N_2$)

3.5 Ultraviolet (UV) degradation

The UV degradation of the specimens was carried out in a UV chamber (S.L.W, 230 V, India) with a mercury arc lamp system that provides a highly uniform UV flux in 200–400 nm range. Specimens were exposed to UV for 0–70 days. The weight loss (%) was calculated as:

weight loss (%) = $(W_t - W_0)/W_0 \times 100$

where 'W_t' is the weight of the sample at time t and 'W_0' is the weight before exposure. The degradation was analyzed using FTIR by measuring the carbonyl (C = O) peaks intensity. The peak heights were decided by deducting the height of the baseline from the total height of the peak. The baseline was kept the same for all the peaks. The following equation was used to calculate the carbonyl index:

Carbonyl index = I_C/I_R,

where I_C is the carbonyl peak intensity (1700 – 1800 cm^{-1}) and I_R is the reference band intensity (2900 – 2950 cm^{-1}) [29, 30]. This peak was taken as a reference due to its minimal change throughout the

exposure. The surface of the UV-degraded samples was analyzed by SEM. Mechanical properties were also studied for the UV exposed specimen.

3.6 Mechanical Properties

The tensile and flexural properties of the composites were investigated using a universal testing machine (Zwick, Z010) at ASTM D-638 and D-790. The average values of three different samples of all varieties were considered.

The hardness of the specimens was determined as per the ASTM D2240 method by employing a durometer (RR12) and denoted as shore D hardness.

3.9 Biodegradation study

The biodegradability of the samples was investigated by employing a UV visible spectrophotometer (Shimadzu Corporation, UV-2450, Japan) at 600 nm against blank culture media.

3.10 Morphological study

The surface of the samples was investigated by employing a scanning electron microscope (JEOL, JSM-6390LV) with a voltage of 5–10 kV. The cracked surface was spluttered with platinum and put on the sample holder.

3.11 Water absorption test

The samples were chopped into pieces (2.5cm×0.5cm×2.5cm) and immersed in water for the test. The weights of the samples were then measured at different time intervals for 0-180h. The equation used to calculate the swelling (%) is:

Swelling (%) = $(W_w - W_0) / W_0 \times 100$

where 'W_w' is the weight of the composites after dipping in water and 'W_0' is the weight before dipping in water.

3.12 Chemical resistance test

The samples were immersed partly in NaOH (4%) and acetic acid (4%) for 1 week. At various time intervals, they were removed, wiped off excess chemicals, and weighed to calculate their percentage weight gain/loss. The equation used to calculate the chemical resistance is:

% Swelling = $(V_f - V_i)/V_i \times 100$

where 'V_i'and 'V_f' is the volume of the samples before and after dipping in the alkali and acid solution.

3.13 Statistical Analysis

One-way analysis of variance (ANOVA) was used to analyze the data statistically and expressed as means ± standard deviation (SD).

4. Results And Discussions

4.1 Fourier Transform Infrared Spectroscopy (FT-IR) of Rosin acid and its derivative

FTIR spectra of the raw material (Rosin acid), intermediate product (MA), and final comonomer (TM) are presented in Fig. 3. The band at 2927 cm^{-1} of the rosin acid spectrum (Fig. 3a) indicated the presence of –CH stretching. The stretching vibration of the carbonyl group of carboxylic acid appeared at 1695 cm^{-1}. The absorption peak at 1284 cm^{-1} was due to the -CO stretching of carboxylic acid. The peaks in the spectrum of maleopimaric anhydride (MA) at 1845 and 1700 cm^{-1} are due to -CO stretching of the anhydride group (Fig. 3a). In the spectrum of TM (Fig. 3b), the peaks at 1650, 985 and 916 cm^{-1} indicated the presence of terminal C = C bonds. The peak that appeared in 1725 cm^{-1} was assigned to the carbonyl group and peaks observed at 2924 and 2849 cm^{-1} were due to the presence of methyl and methylene groups.

4.2 Fourier Transform Infrared Spectroscopy (FT-IR) of Chicken feather and biocomposites

FTIR spectra of the chicken feather and the composites loaded with varying percentages of rosin acid derivative are presented in Fig. 4. Chicken feather fiber (curve a) showed characteristic absorption bands at 3290 cm^{-1} corresponding to N-H symmetric amide stretching. The peaks at 2962 and 2930 cm^{-1} observed were due to asymmetric and symmetric stretching vibrations of methyl (CH_3) in keratin protein. The peaks at 1652 and 1534 cm^{-1} were due to –C = O symmetrical stretching of amide (I) and N-H bending vibration of amide (II). The absorption band that appeared at 710 cm^{-1} was due to alkyl thiols (C-S), which originated from the amino acid cysteine. In the FT-IR spectra of composites (curve b-e), loaded with different percentages of TM, the intensity of the N-H peak that appeared for chicken feather at 3290cm^{-1} was found to be decreased and ultimately almost diminished in all the composites.

In all the composites, the C = C stretching peak of TM was shifted from 1650 cm^{-1} to 1638 cm^{-1} (curve c), and 1633 cm^{-1} (curve d, e), and the intensity of the peaks were found to reduce. Also the C = O stretching peak appeared at 1725 cm^{-1} for MAESO/CF/TM0 (curve b) was found to shift to 1720 cm^{-1}, 1716 cm^{-1} and 1715 cm^{-1} for the samples MAESO/CF/TM20, MAESO/CF/TM30 and MAESO/CF/TM40 respectively. The peaks corresponding to asymmetric and symmetric stretching of CH_3 were shifted to lower wave numbers. It was observed that the C = O peak intensity got reduced after the incorporation of TM in the formulations. The reduction in peak intensities and shifting of the peaks indicated a better interaction and formation of crosslinked structure among all the components of the composites.

4.3 Density Functional Theory (DFT) Study

DFT study was carried out for all the components involved in the synthesis of the cross-linker product MAESO/TM/CF as shown in Fig. 2. Structures of the reactants were optimized following the information gathered from available literature based on the crystal structure. A probable cross-linked structure has been reported for the resultant product also supported by the DFT calculations. Optimized structures of Rosin acid, MAESO, TM, CF, and a unit of the cross-linked product (MAESO/TM/CF) are shown in Fig. 5. and Fig. 6. Hessian calculations exhibited absence of negative imaginary frequencies, which indicated the optimized structures to be true minima on the potential energy surface. The cross-linked product MAESO/TM/CF composite consists of hydroxyl, epoxy, and carbonyl functional groups. The calculated vibrational frequencies of the important functional groups are listed in Table 2 and were in accordance with the experimental values obtained from FTIR spectroscopy (Figs. 3 and 4).

Table 2
Experimental and theoretical infrared spectral data of the optimized complexes

Name Code	Functional Groups		Frequencies (cm^{-1})
Rosin acid	-CH stretching	Exp.	2953
		Calc	2927
	-C = O stretching	Exp.	1789
		Calc	1695
	-C-O stretching	Exp.	1291
		Calc	1284
TM	-CH stretching	Exp.	2980
		Calc	2924
	-C = O stretching	Exp.	1735
		Calc	1725
	-C = C (terminal)	Exp.	1706
		Calc	1650
	-C-O stretching	Exp.	1223
		Calc	1231
MAESO/TM/CF	-CH stretching	Exp.	2991
		Calc	2962
	-C = O stretching	Exp.	1801 – 1734
		Calc	1725 – 1715
	-C = C (terminal)	Exp.	1700 – 1683
		Calc	1650 – 1633

4.4 Thermogravimetric analysis (TGA)

The thermal property of the composites was investigated by TGA. Table 3 presents the initial decomposition temperature (Ti), maximum pyrolysis temperature (Tm), and residual weight (%) of the specimen. The values presented (Table 3) were the average of three different samples. After incorporation of rosin derivative into the composites the Ti values increases. Rosin derivative played a remarkable role in improving the thermal properties as it could enhance the interaction between the resin and chicken

feather fibers and thereby restricted the mobility of volatile degraded products out of the crosslinked network structure. Samples with 30 wt% of TM (MAESO/CF/TM30) showed maximum thermal resistance. The lower thermal resistance shown by the composite prepared with 40 wt% of TM (MAESO/CF/TM40) was due to the presence of higher amount of TM which might have lowered the interaction among the constituents of the composites. The residual weight percentage of the composite loaded with 30 wt% of TM was found to be maximum due to char formation on the surface while exposed to heat and blocking the air to penetrate into the composites. The formation of highest amount of char was as a consequence of the development of an improved crosslinked structure produced by the interaction between CF, resin, and TM.

Table 3
Thermal analysis of the composites

Samples	Initial decomposition temperature (°C) (T_i)	Maximum pyrolysis temperature (°C) (T_m)		Temperature of decomposition (°C) (T_d) at different weight loss (%)				Residual weight (%) at 600°C
		1st step	2nd step	20%	40%	60%	80%	
CF	225	288	308	262	311	407	572	13
MAESO/CF/TM0	211	370	411	296	355	405	585	18
MAESO/CF/TM20	231	371	414	294	357	406	582	18
MAESO/CF/TM30	234	367	414	297	357	408	-	20
MAESO/CF/TM40	221	297	393	279	328	410	527	16

4.5 Limiting Oxygen Index (LOI) study

The LOI values of the composites loaded with varying amounts of TM are presented in Table 4. The values were found to increase after the inclusion of TM up to 30wt% and after that, the values decreased beyond that percentage. The increase in values might be due to the participation of the phenanthrene ring of TM to form a crosslinked structure between resin, CF, and TM. Also, it provided a thermal barrier promoting char formation and thus enhanced the thermal stability of the prepared composites. Char shielded the surface of the samples from heat and lowered the loss of mass rate in the course of thermal decomposition, thus giving an enhanced flame resistivity. At a higher percentage of TM, the LOI values decreased which might be due to weak interaction among the constituents of the composites.

Table 4
Limiting Oxygen Index (LOI) test of the composites

Samples	LOI (%)	Flame Description	Smokes and Fumes	Char
MAESO/CF/TM0	38	Small localized flame	Dark Fumes	Medium
MAESO/CF/TM20	44	Small localized flame	Dark Fumes	Medium
MAESO/CF/TM30	55	Small localized flame	Dark Fumes	Medium
MAESO/CF/TM40	50	Small localized flame	Dark Fumes	Medium

4.6 Ultraviolet resistance test

Figure 7. represents the weight loss of the samples prepared with varying percentages of TM which were subjected to a UV environment for several days. In all the samples, with or without TM, weight loss % was found to be increased initially due to moisture absorption. The loss in the material due to degradation was minimal than the initial decrease in loss in weight of the samples. The sample without TM showed highest weight loss (%) followed by the TM loaded samples after 70 days of irradiation. After the incorporation of TM, the rate of weight loss decreased. Composite loaded with 30 wt% of TM showed minimum weight loss. This might be due to interaction among chicken feather fiber, resin, TM leading to the formation of a crosslinked structure which slowed down the photodegradation method and enhanced the UV resistance.

Figure 8. shows the FTIR spectra of UV exposed samples which were investigated by the shifting in the intensities of carbonyl peak. In all the composites, the –OH stretching peak appeared in the 3455 – 3450 cm^{-1} range. The peaks between 2932 – 2927 cm^{-1} were due to –CH stretching. It was observed that the intensity of the carbonyl peak at 1726 cm^{-1} was more for the composite without rosin acid derivative. However, after the incorporation of rosin acid derivative, the intensity of the carbonyl peak decreased and shifted to 1725 cm^{-1} and 1720 cm^{-1} respectively indicating the formation of a better crosslinked structure and thus imposing restriction on the composites from photodegradation.

The change in carbonyl index values of the composites with/without rosin derivative after 70 days of UV exposure are shown in Fig. 9. Composite with rosin derivative (MAESO/CF/TM0) showed more carbonyl index values compared to the composites loaded with rosin acid derivative. The increase in carbonyl index values was could be because of chain scission between the matrix and the fiber. The carbonyl value index decreased up to the 30 wt% addition of rosin derivative after that it increased. The rosin derivative might have stabilized the composites by protecting them from UV radiation and slowed down the process of photodegradation. Similar UV stability of wood polymer composite was reported by Mandal et al. [29]. However, at 40 wt% of rosin derivative loading (MAESO/CF/TM40), the carbonyl index values increased. The reason might be due to excess amount of TM leading to weak interaction between the constituents of the composites.

4.7 Mechanical property

The mechanical and hardness values of the composites with various percentages of TM before and after UV exposure are presented in Table 5. The addition of TM into the composites contributed immensely to the tensile, flexural, and hardness strength. Composites loaded with 30wt% of TM showed maximum values and beyond that, the values decreased. The enhancement in the mechanical properties could be due to enhanced interaction among the CF, TM, and resin. Also, the existence of a large phenanthrene ring in the TM provided stiffness to the composites. The decrease in mechanical properties might be due to the presence of the unreacted components in the composites which resulted in poor adhesion among the chicken feather fiber based polymer composites.

Table 5 also shows the mechanical properties of the UV degraded composites after 70 days of irradiation. The results shows reduced tensile, flexural, and hardness values of the composites. Highest loss in all the properties was observed for the composites without TM. However, the loss was less significant in the composites having various percentages of TM. The minimal loss in the properties of the specimens was could be the consequence of enhanced crosslinked structure between the TM, CF, and resin. Further, the presence of TM might have delayed the photodegradation process offering resistance to the composites.

Table 5
Mechanical properties of the composites before and after UV degradation study

Samples	Tensile Strength (MPa)		Flexural strength (MPa)		Hardness (Shore D)	
	Before	After	Before	After	Before	After
MAESO/CF/TM0	10.05 (± 0.46)	6.82 (± 0.98)	29.68 (± 1.67)	23.4 (± 0.79)	71.6 (± 1.52)	67.33 (± 1.52)
MAESO/CF/TM20	10.26 (± 1.09)	7.31 (± 0.99)	30.03 (± 1.12)	26.42 (± 0.57)	74.66 (± 0.5)	71.6 (± 1.60)
MAESO/CF/TM30	13.97 (± 0.93)	10.35 (± 1.01)	37.80 (± 0.79)	33.25 (± 0.99)	80.33 (± 1.52)	77.8 (± 0.76)
MAESO/CF/TM40	12.71 (± 0.65)	9.67 (± 1.27)	32.41 (± 0.78)	28.33 (± 0.66)	77 (± 1.32)	73.33 (± 1.60)

4.8 Biodegration study

Figure 10. shows the bacterial growth studied for four weeks on the composites loaded with various percentages of TM, *Bacillus cereus* and *Pseudomonas aeruginosa* were used for biodegradation of the samples. The bacterial growth and degradation rate in the broth culture medium containing mineral salts and samples as a sole carbon source were evident after one week of incubation. The bacterial growth

was found to be enhanced steadily with rise in the time of the bacterial exposure. In the sample loaded with 30 wt% of TM, initially, the bacterial growth was exponential and then it became stationary (no further increase in growth over time), and for the composites loaded with 20 and 40 wt% of TM, the bacterial growth was found to be higher but decreased after two weeks of incubation, possibly due to accumulation of inhibitory by-products produced by the microorganism. The degradation pattern in the case of the composite without TM was found to increase till four weeks of incubation. The high rate of degradation of the samples could be attributed to the hydrolytic enzyme production (including keratinases and proteases) capability of the bacterium *Bacillus cereus* and *Pseudomonas aeruginosa* that could degrade the proteins present in the chicken feather. Several studies reported the production of keratinases and peptidases by *Bacillus* sp. (including *Bacillus cereus* and *B. licheniformis*) using chicken feather as the sole carbon and nitrogen source [31–33]. Samples loaded with 20 and 40 wt% of TM showed higher degradation than 30 wt% TM loaded samples probably due to lower crosslinking among the components of the composites [34].

4.9 Morphological analysis

The SEM micrographs of the composites with/without rosin derivative are shown in Fig. 11. Voids and surface roughness appeared in the composites without TM (MAESO/CF/TM0). From the SEM images, it is evident that the surface roughness of the samples decreased after the incorporation of TM. With the increase in the TM percentage up to 30 wt%, the void spaces and surface roughness were found to decrease implying an enhanced interaction and compatibility among the constituents of the composites. However, in the composite loaded with 40 wt% of TM (MAESO/CF/TM40), the surface was found to be uneven due to aggregation of excess amount of TM. The composites were exposed to UV rays for 70 days. The SEM micrographs of the samples exposed to UV are shown in Fig. 12. It could be observed that due to photodegradation cracks appeared on the surface of the composites and surface roughness increased. The surface of the composite without TM (MAESO/CF/TM0) appeared rougher than the composites with TM. The addition of TM into the composites retarded the development of cracks onto the bulk of the composites. The rosin derivative promoted the interaction among the resin, CF, and TM which in turn minimized the degradation of the composites against UV rays.

Figure 13. shows the SEM micrographs of the degraded samples caused by bacterial growth. Physical breakdown of the composites without TM compared to the composites loaded with TM after the microbial attack was evident from the images. It was also observed that the areas where fibers were exposed were partially damaged whereas those deeply embedded in the matrix are unaffected. The decrease in degradation of composites with TM was due to the formation of a strongly interconnected network which lowered the accessibility and reactivity of the microorganisms. The SEM image of the composite loaded with 30 wt% of TM (MAESO/CF/TM30) showed minimum cracks compared to the other composites which revealed the influence of TM on the rate of degradation of the composites.

4.10 Water absorption test

The water uptake of the composites is shown in Fig. 14. The water uptake capacity was very high in the beginning and later it reduced for all the samples. Water uptake was found to be less for the composites loaded with TM compared to unloaded composites. The existence of the phenanthrene ring structure of TM and the crosslinked network in the composites might be the reason which inhibited the inflow of water thoroughly into the samples and hence significantly reduced the water absorption value. Composite loaded with 30 wt% of TM (MAESO/CF/TM30) showed the least swelling. The swelling again increased for the composite loaded with 40 wt% of TM (MAESO/CF/TM40), which might be due to the presence of an excessive quantity of TM in the polymer matrix leading to weak interaction among the constituents of the composites followed by collapsing of the network structure.

4.11 Chemical Resistance Test

Figure 15. shows the chemical resistance test for the composites which were carried out in 4% acetic acid and 4% NaOH solution. In all the samples, swelling increased with increase in time. Highest swelling was shown by the composite prepared without rosin derivative. The swelling was found to decrease after the incorporation of rosin derivative which helps to form the crosslinked structure and thus decreases the accessibility of chemicals into the samples. It was also observed that composites were more resistive in acid solution than in alkali solution. The higher swelling in alkali solution might be due to enhanced interaction between NaOH, chicken feather, resin, and TM. Both the acid and alkali solution composite with 30 wt% of TM (MAESO/CF/TM30) showed least swelling. The composite containing 40 wt% of TM (MAESO/CF/TM40) showed less resistance to chemicals due to the dilution effect leading to weak interaction between the constituents of the composites.

5. Conclusion

In this work, a biodegradable chicken feather based composite was prepared successfully using rosin derivative as a crosslinker and modified epoxidized soybean oil as resin. The use of biobased as well as renewable resources to develop the composites has provided a new way to minimize the employment of petroleum based substances, which also contributes to solid waste management by serving as an alternative to the traditional composite industry. FTIR study was carried out to confirm the chemical structure of rosin acid and its derivative. FTIR study also displayed the possible interaction among the constituents of the composites. The results were further favored by the DFT study. Considerable improvement in the thermal and mechanical properties was seen after the inclusion of rosin acid derivative. Properties like water uptake, chemical resistance, biodegradability, flame retardancy were found to be improved after the incorporation of rosin acid derivative. The surface of the composites was analyzed by SEM study. The UV resistance was found to be improved in the composites loaded with rosin derivative as indicated by weight loss, carbonyl index, SEM, and reduced mechanical properties values. The rosin derivative can impressively behave as a shield for the biocomposites by elevating the UV stability. The enhancement in overall properties was more in the samples loaded with 30 wt% of TM. Thus the obtained composites can be considered as future generation products with minimum cost and

having maximum properties leading to waste minimization. These composites can be used for a variety of purposes ranging from structural applications to household products.

Declarations

Conflict of interest

The authors declare that there is no conflict of interests regarding the publication of this paper.

Acknowledgment

The author, Gitashree Gogoi greatly acknowledged University Grants Commission (UGC), New Delhi, for providing Financial assistance (as a fellowship). Grant number- NFO-2018-19- OBC-ASS-75119.

References

1. Campanella A, Wool RP, Bah M, Fita S, Abuobaid A (2013) Composites from northern red oak (Quercus robur) leaves and plant oil-based resins. J Appl Polym Sci 127:18–26. doi:10.1002/app.36663
2. Lau AKT, Cheung KHY (2017) Natural fiber-reinforced polymer-based composites. Elsevier Ltd. doi: 10.1016/B978-0-08-100656-6.00001-7
3. Thakur VK, Singha AS, Thakur MK (2013) Green composites from natural fibers: Mechanical and chemical aging properties. Int J Polym Anal 17:401–407. doi: 10.1080/1023666X.2012.668665
4. Reddy N (2015) Non-food industrial applications of poultry feathers. Waste Manag 45:91–107. doi: 10.1016/j.wasman.2015.05.023
5. Bansal G, Singh VK (2016) Review on Chicken Feather Fiber (CFF) a Livestock Waste in Composite Material Development. Int J Waste Resour 06:16–24. doi: 10.4172/2252-5211.1000254
6. Tesfaye T, Sithole B, Ramjugernath D, Mokhothu T (2018) Valorisation of chicken feathers: Characterisation of thermal, mechanical and electrical properties. Sustain Chem Pharm 9:27–34. doi: 10.1016/j.scp.2018.05.003
7. Acda MN (2010) Waste chicken feather as reinforcement in cement-bonded composites. Philipp J Sci 139:161–166
8. Hong CK, Wool RF (2005) Development of a bio-based composite material from soybean oil and keratin fibers. J Appl Polym Sci 95:1524–1538. doi: 10.1002/app.21044
9. Aranberri I, Montes S, Azcune I, Rekondo A, Grande HJ (2017) Fully biodegradable biocomposites with high chicken feather content. Polym (Basel) 9. doi:10.3390/polym9110593
10. Doineau E, Coqueugniot G, Pucci MF, Caro AS, Cathala B, Bénézet JC et al (2021) Hierarchical thermoplastic biocomposites reinforced with flax fibres modified by xyloglucan and cellulose nanocrystals. Carbohydr Polym 254. doi: 10.1016/j.carbpol.2020.117403

11. Yang Z, Peng H, Wang W, Liu T (2010) Crystallization behavior of poly(ε-caprolactone)/layered double hydroxide nanocomposites. J Appl Polym Sci 116:2658–2667. doi: 10.1002/app
12. Saithai P, Lecomte J, Dubreucq E, Tanrattanakul V (2013) Effects of different epoxidation methods of soybean oil on the characteristics of acrylated epoxidized soybean oil-co-poly(methyl methacrylate) copolymer. Express Polym Lett 7:910–924. doi: 10.3144/expresspolymLett.2013.89
13. Khot SN, Lascala JJ, Can E, Morye SS, Williams GI, Palmese GR et al (2001) Development and application of triglyceride-based polymers and composites. J Appl Polym Sci 82:703–723. doi: 10.1002/app.1897
14. Habib F, Bajpai M (2011) Synthesis and Characterization of Acrylated Epoxidized Soybean Oil for Uv Cured Coatings. Chem Chem Technol 5:317–326
15. Mustapha SNH, Rahmat AR, Arsad A (2014) Bio-based thermoset nanocomposite derived from vegetable oil: A short review. Rev Chem Eng 30:167–182. doi: 10.1515/revce-2013-0010
16. Ma Q, Liu X, Zhang R, Zhu J, Jiang Y (2013) Synthesis and properties of full bio-based thermosetting resins from rosin acid and soybean oil: The role of rosin acid derivatives. Green Chem 15:1300–1310. doi: 10.1039/c3gc00095h
17. Liu Y, Li C, Dai JY, Jiang YH, Liu XQ, Zhu J (2017) Synthesis of multifunctional monomers from rosin for the properties enhancement of soybean-oil based thermosets. Sci China Technol Sci 60:1332–1338. doi: 10.1007/s11431-016-0777-5
18. Liu X, Xin W, Zhang J (2009) Rosin-based acid anhydrides as alternatives to petrochemical curing agents. Green Chem 11:1018–1025. doi: 10.1039/b903955d
19. Lin R, Li H, Long H, Su J, Huang W (2014) Synthesis of rosin acid starch catalyzed by lipase. Biomed Res Int 2014. doi: 10.1155/2014/647068
20. Mustata FR, Tudorachi N (2010) Epoxy resins cross-linked with rosin adduct derivatives. Cross-linking and thermal behaviors. Ind Eng Chem Res 49:12414–12422. doi: 10.1021/ie101746v
21. Liu X, Xin W, Zhang J (2010) Rosin-derived imide-diacids as epoxy curing agents for enhanced performance. Bioresour Technol 101:2520–2524. doi: 10.1016/j.biortech.2009.11.028
22. Liu XQ, Huang W, Jiang YH, Zhu J, Zhang CZ (2012) Preparation of a bio-based epoxy with comparable properties to those of petroleum-based counterparts. Express Polym Lett 6:293–298. doi: 10.3144/expresspolymLett.2012.32
23. Gogoi G, Mandal M, Maji TK (2019) Study of Properties of Modified Soybean Oil Based Composite Reinforced with Chicken Feather. Fibers Polym 20:1061–1068. doi: 10.1007/s12221-019-8843-x
24. Frisch MJEA, Trucks GW, Schlegel HB, Scuseria GE, Robb MA, Cheeseman JR, Scalmani G, Barone V, Mennucci B, Petersson G, Nakatsuji H (2009) gaussian 09, Revision d, vol 01. Gaussian Inc, Wallingford CT, p 201
25. You A, Be MAY, In I (2003) Self — Consistent Molecular Orbital Methods. XII. Further Extensions of Gaussian — Type Basis Sets for Use in Molecular Orbital Studies of Organic Molecules.J Chem Phys284

26. Hariharan PC, Pople JA (1973) The influence of polarization functions on molecular orbital hydrogenation energies. Theor Chim Acta 28:213–222. doi: 10.1007/BF00533485
27. Andersson MP, Uvdal P (2005) New scale factors for harmonic vibrational frequencies using the B3LYP density functional method with the triple-ζ basis set 6-311 + G (d, p). J Phys Chem A 109:2937–2941
28. Takano Y, Houk KN (2005) Benchmarking the conductor-like polarizable continuum model (CPCM) for aqueous solvation free energies of neutral and ionic organic molecules. J Chem Theory Comput 1:70–77. https://doi.org/10.1021/ct049977a
29. Mandal M, Bardhan P, Mandal M, Maji TK (2020) Study of UV stability, biodegradability and physical properties of rosin derivative cross-linked wood polymer composites. Int Wood Prod J 11:2–11. https://doi.org/10.1080/20426445.2019.1706136
30. Taylor P, Hazarika A, Maji TK (2015) Ultraviolet resistance and other physical properties of softwood polymer nanocomposites reinforced with ZnO nanoparticles and nanoclay. Wood Mater Sci Eng 37–41. doi: 10.1080/17480272.2014.992471
31. Peng Z, Mao X, Zhang J, Du G, Chen J (2019) Effective biodegradation of chicken feather waste by co-cultivation of keratinase producing strains. Microb Cell Fact 18:1–11. doi: 10.1186/s12934-019-1134-9
32. Brandelli A, Sala L, Kalil SJ (2015) Microbial enzymes for bioconversion of poultry waste into added-value products. Food Int 73:3–12. doi: 10.1016/j.foodres.2015.01.015
33. Mazotto AM, de Melo ACN, Macrae A, Rosado AS, Peixoto R, Cedrola SML et al (2011) Biodegradation of feather waste by extracellular keratinases and gelatinases from Bacillus spp. World J Microbiol Biotechnol 27:1355–1365. doi: 10.1007/s11274-010-0586-1
34. Mandal M, Bardhan P, Mandal M, Maji TK (2020) Development of wood polymer composites with thermosetting resin from soybean oil cross-linked with rosin derivative. Eur J Wood Prod 78:1265–1278. doi: 10.1007/s00107-020-01564-3

Figures

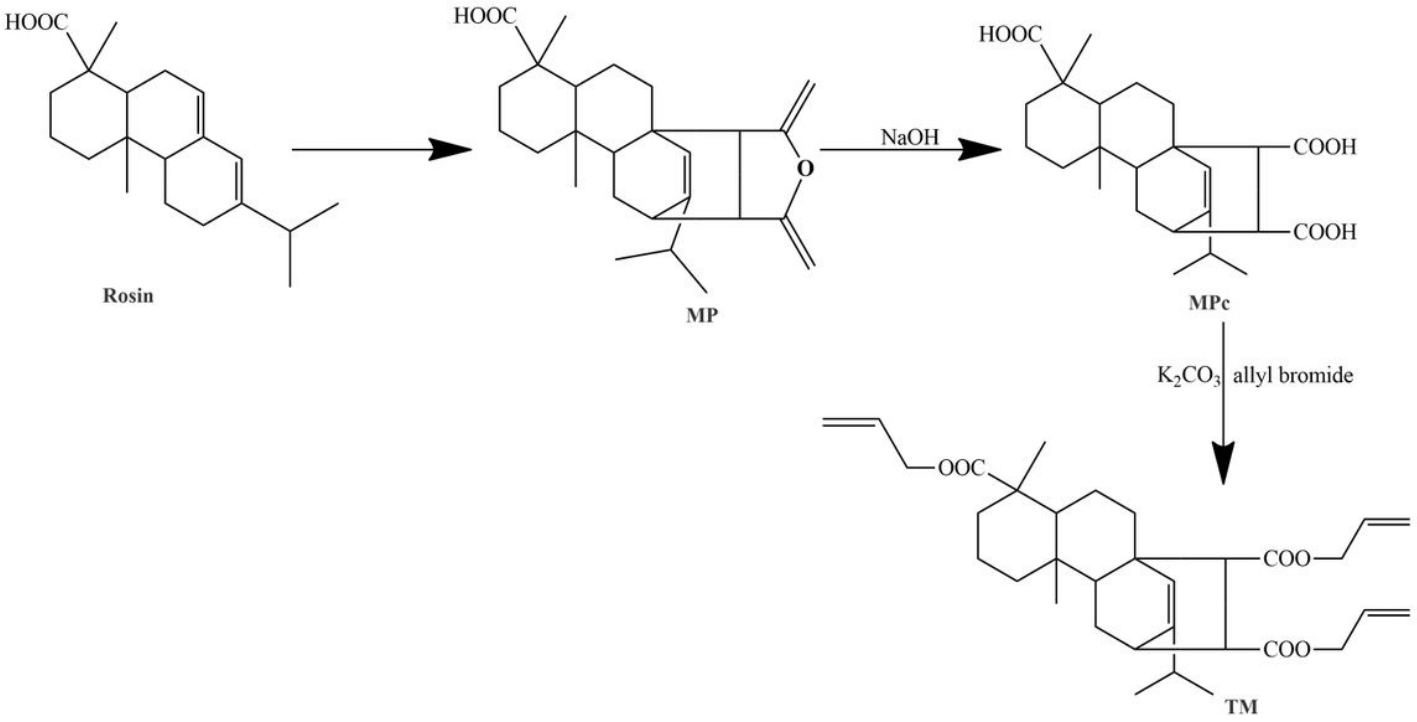

Figure 1

Reaction scheme for the synthesis of triallyl rosin (TM) from rosin acid

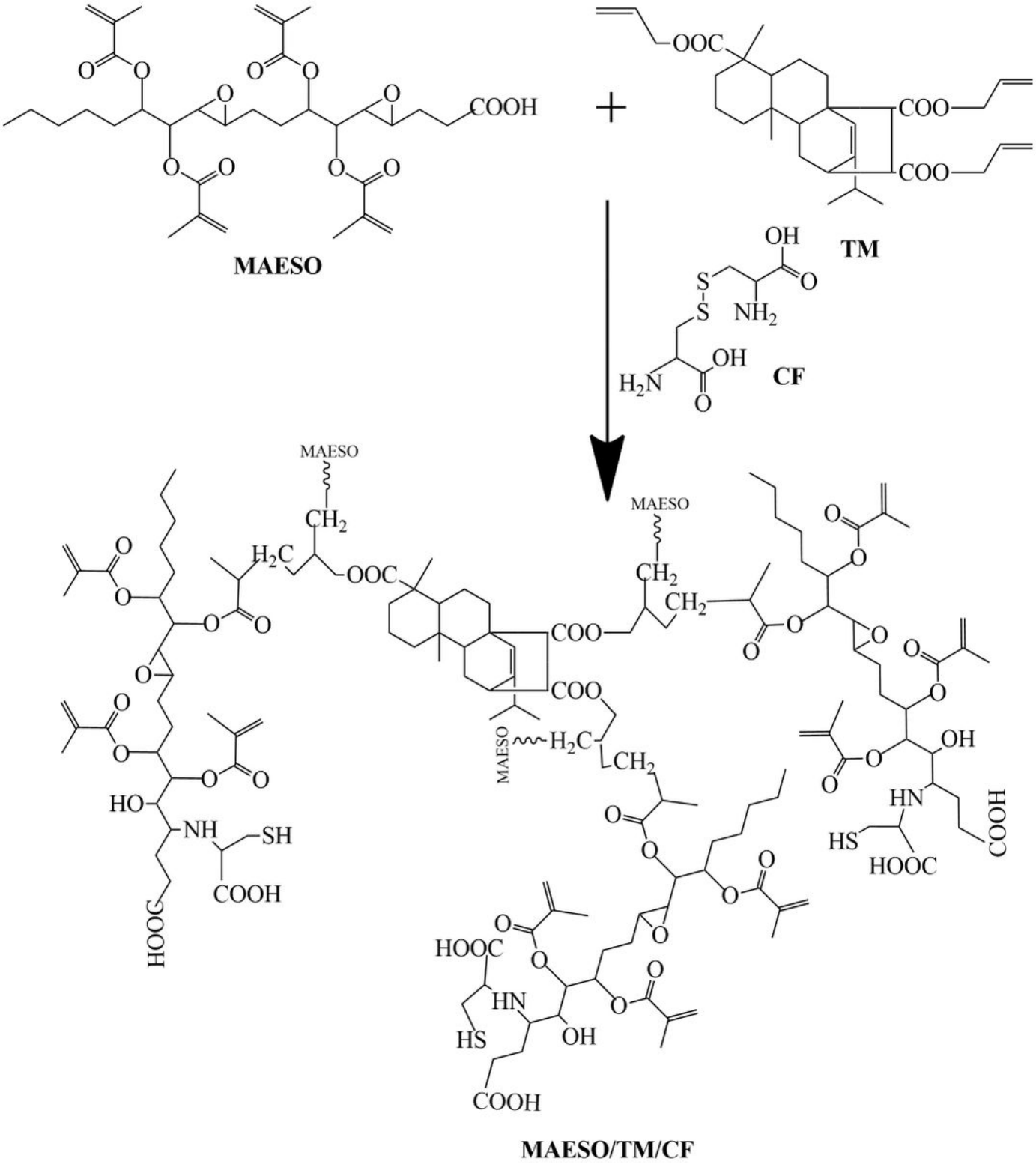

Figure 2

Probable crosslinked structure of the composites

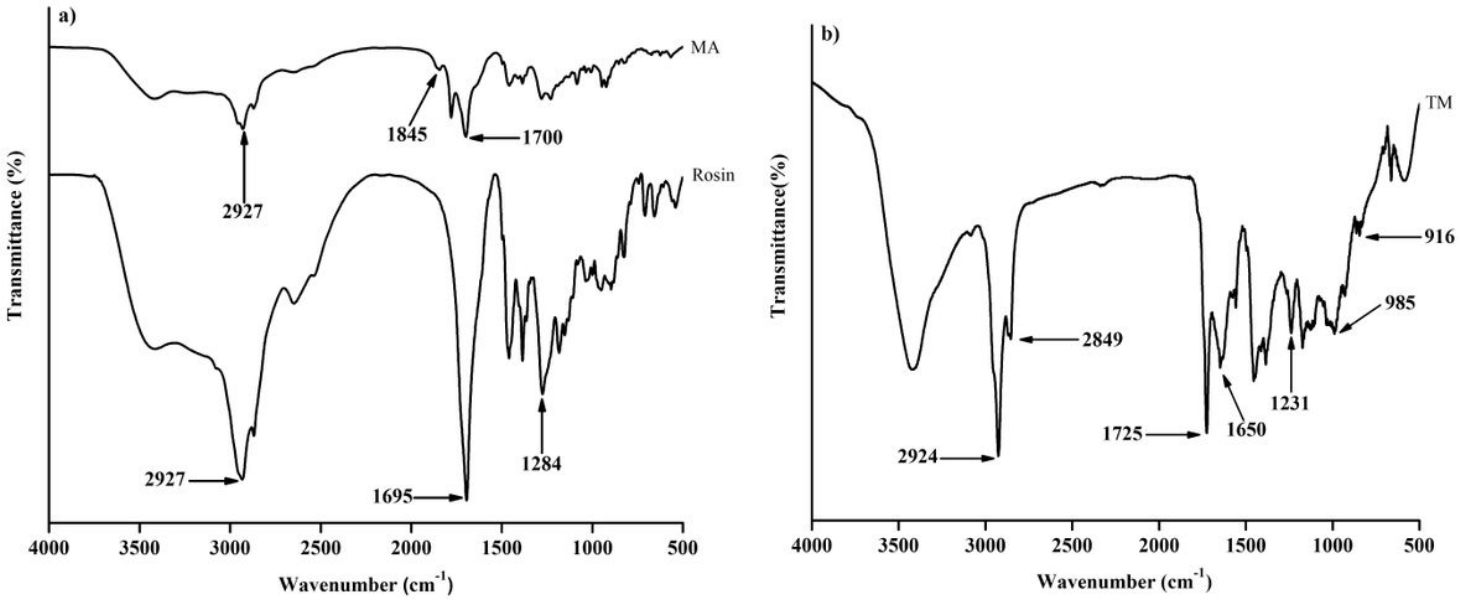

Figure 3

a) FTIR spectra of (a) Rosin acid (b) Maleopimaric anhydride (MA) b) FTIR spectra of (a) Triallyl maleopimarate (TM)

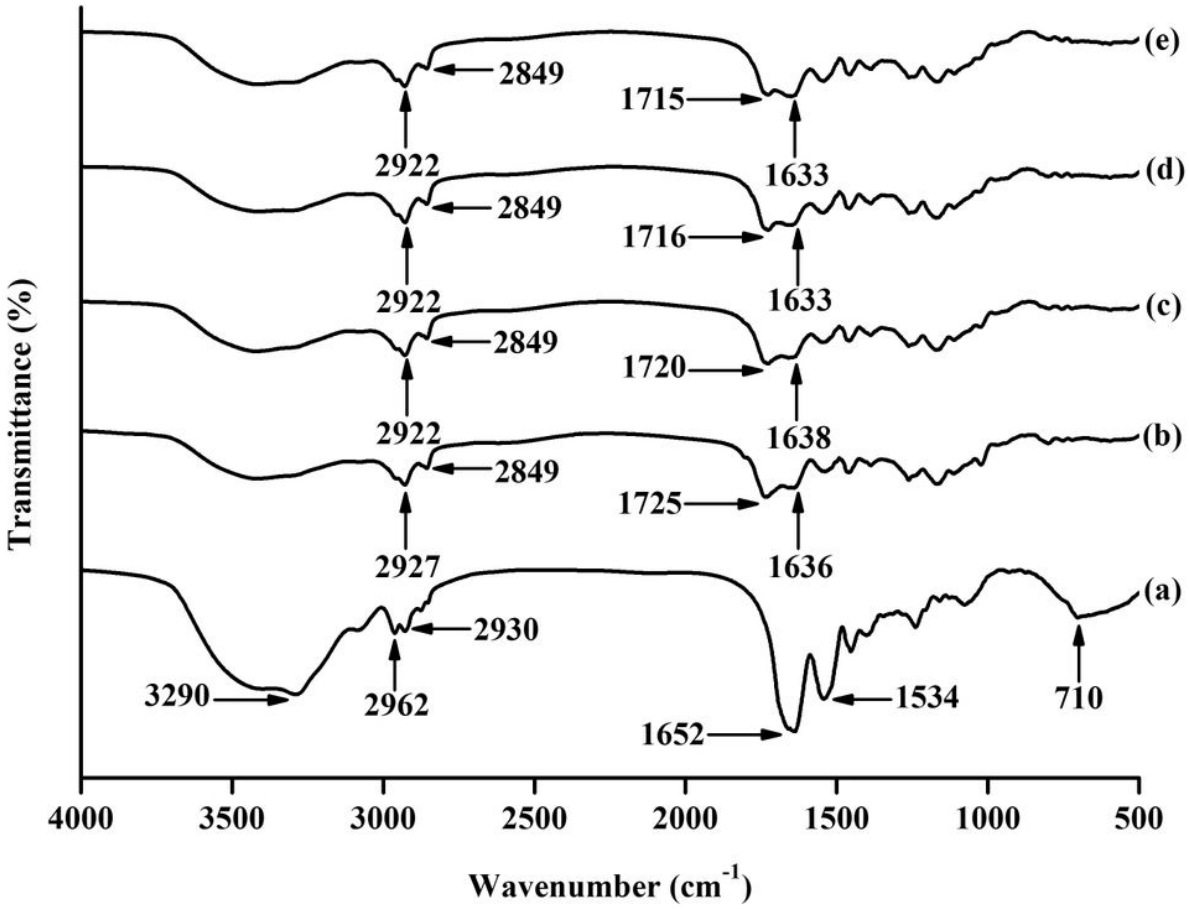

Figure 4

FTIR spectra of a) CF b) MAESO/CF/TM0 c) MAESO/CF/TM20 d) MAESO/CF/TM30 e) MAESO/CF/TM40

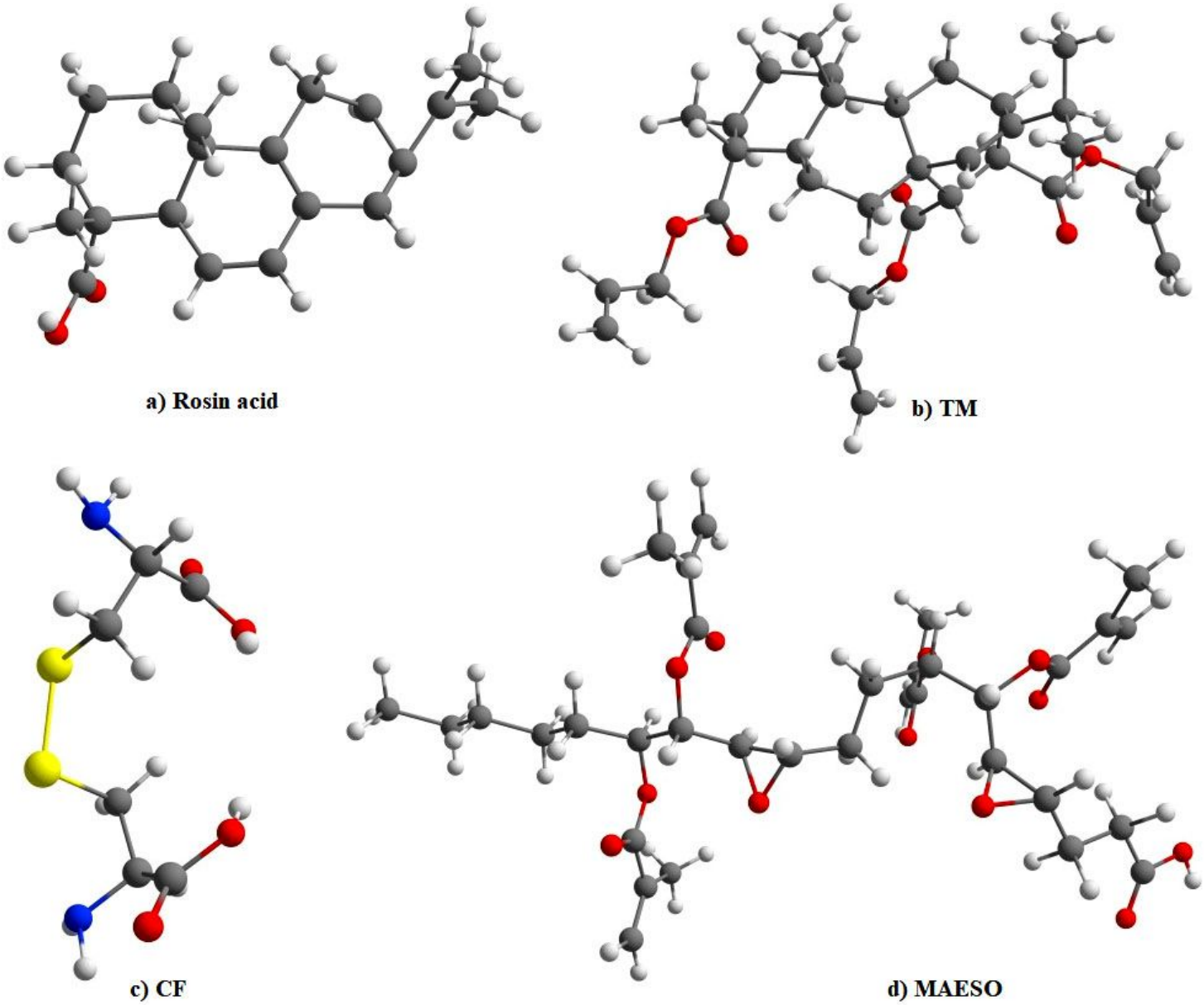

Figure 5

DFT optimized structures of different reactants

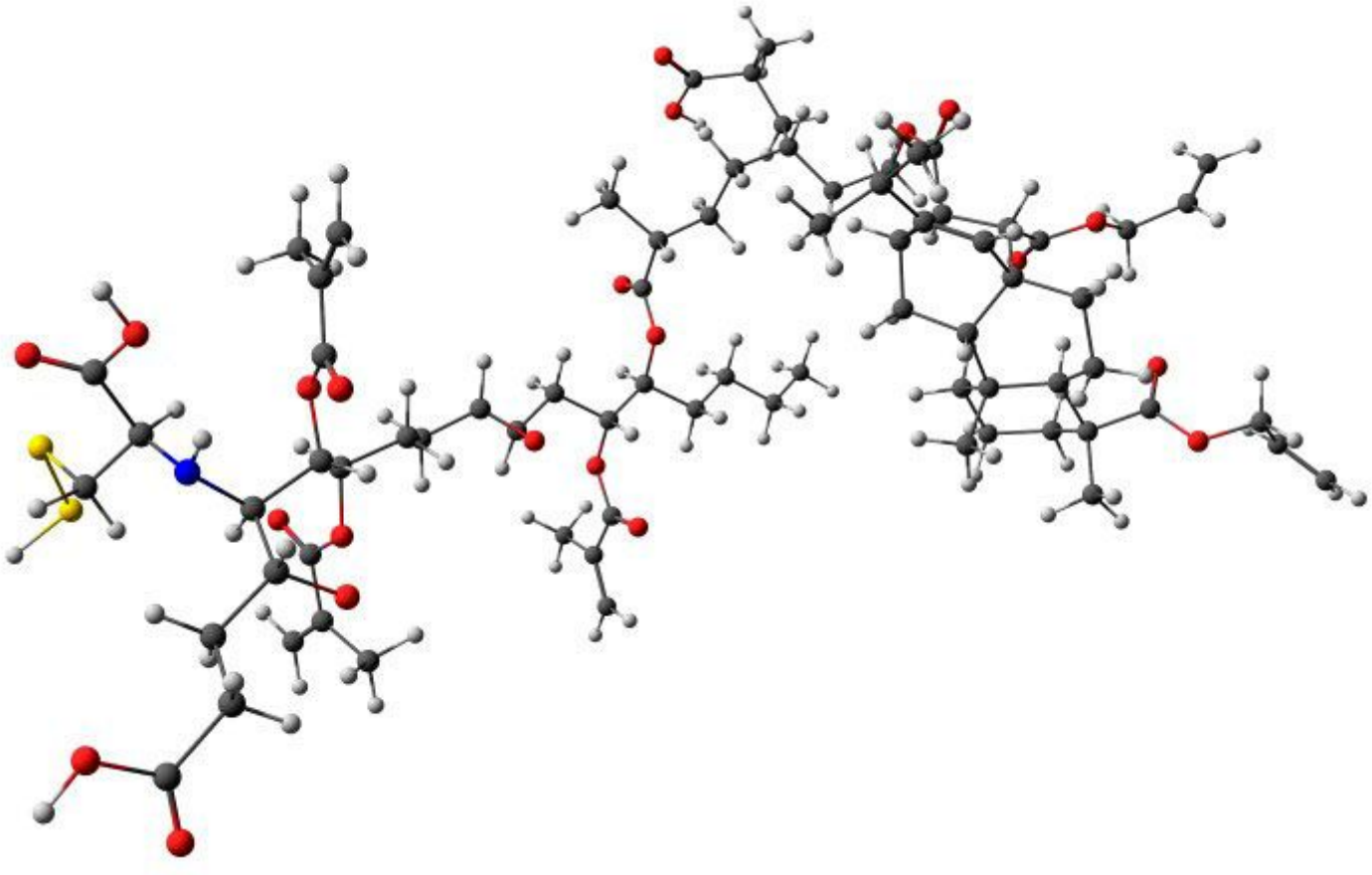

Figure 6

DFT optimized structure of the probable crosslinked MAESO/TM/CF

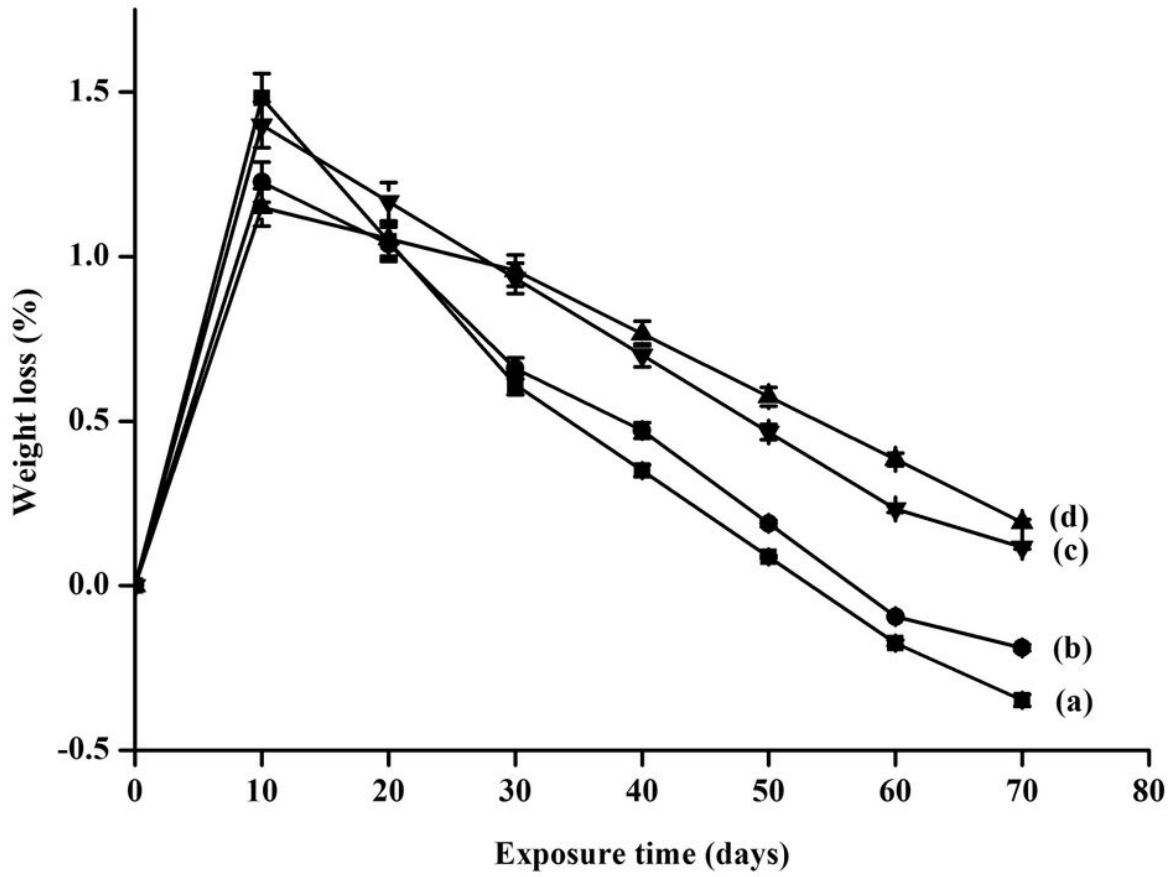

Figure 7

Weight loss versus exposure time of UV exposed composites: a) MAESO/CF/TM0 b) MAESO/CF/TM20 c) MAESO/CF/TM40 d) MAESO/CF/TM30

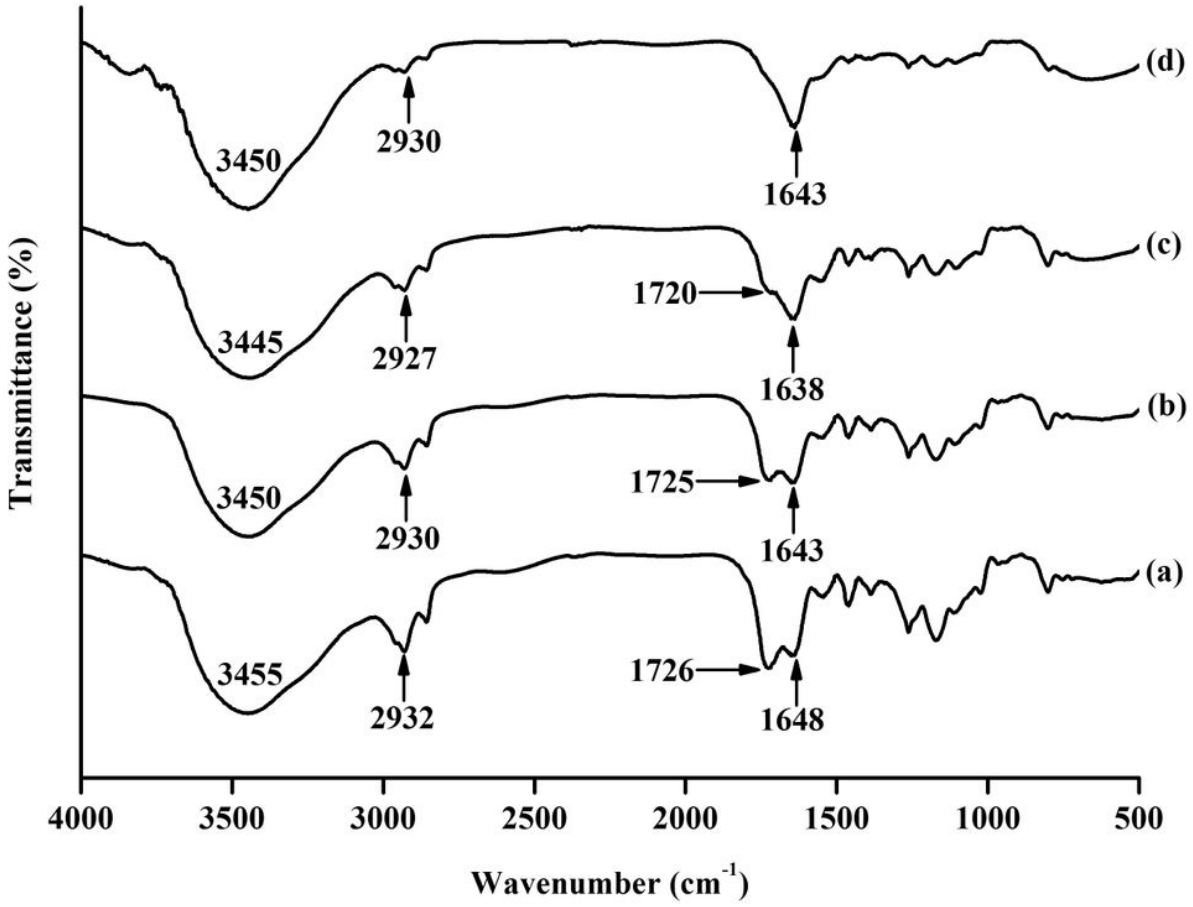

Figure 8

FTIR spectra of UV exposed samples a) MAESO/CF/TM0 b) MAESO/CF/TM20 c) MAESO/CF/TM30 d) MAESO/CF/TM40

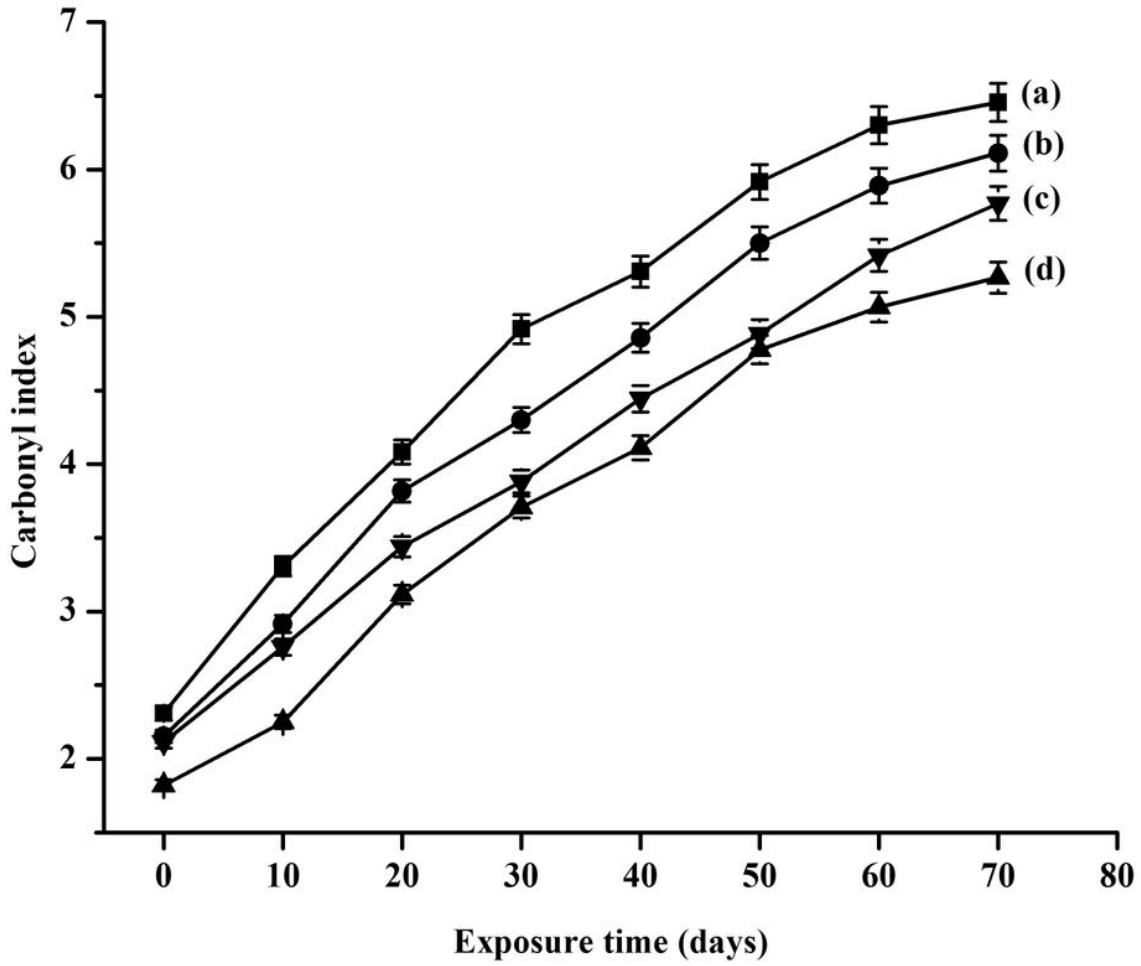

Figure 9

Carbonyl index values of a) MAESO/CF/TM0 b) MAESO/CF/TM20 c) MAESO/CF/TM40 d) MAESO/CF/TM30

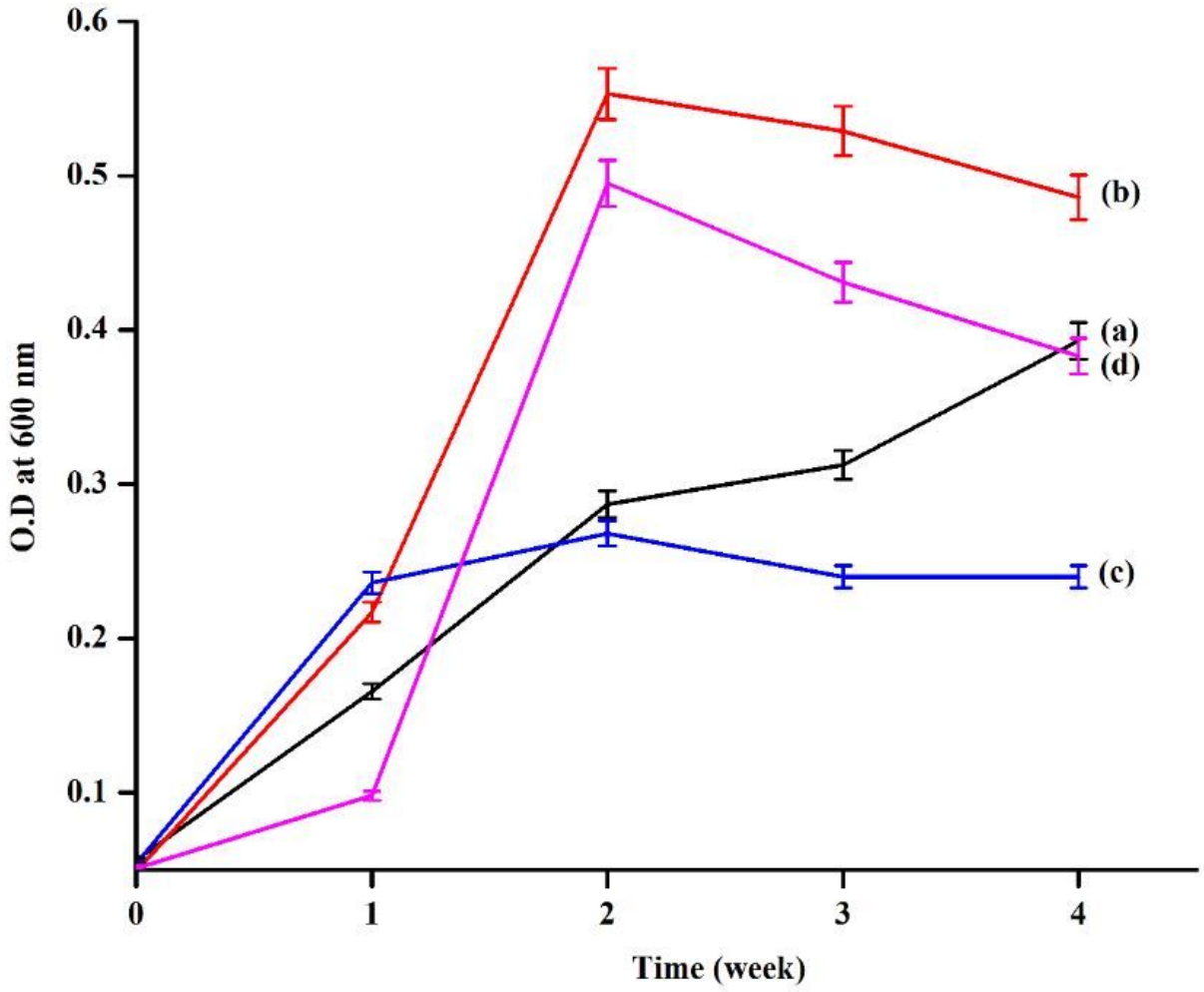

Figure 10

Bacterial growth on a) MAESO/CF/TM0 b) MAESO/CF/TM20 c) MAESO/CF/TM40 d) MAESO/CF/TM30

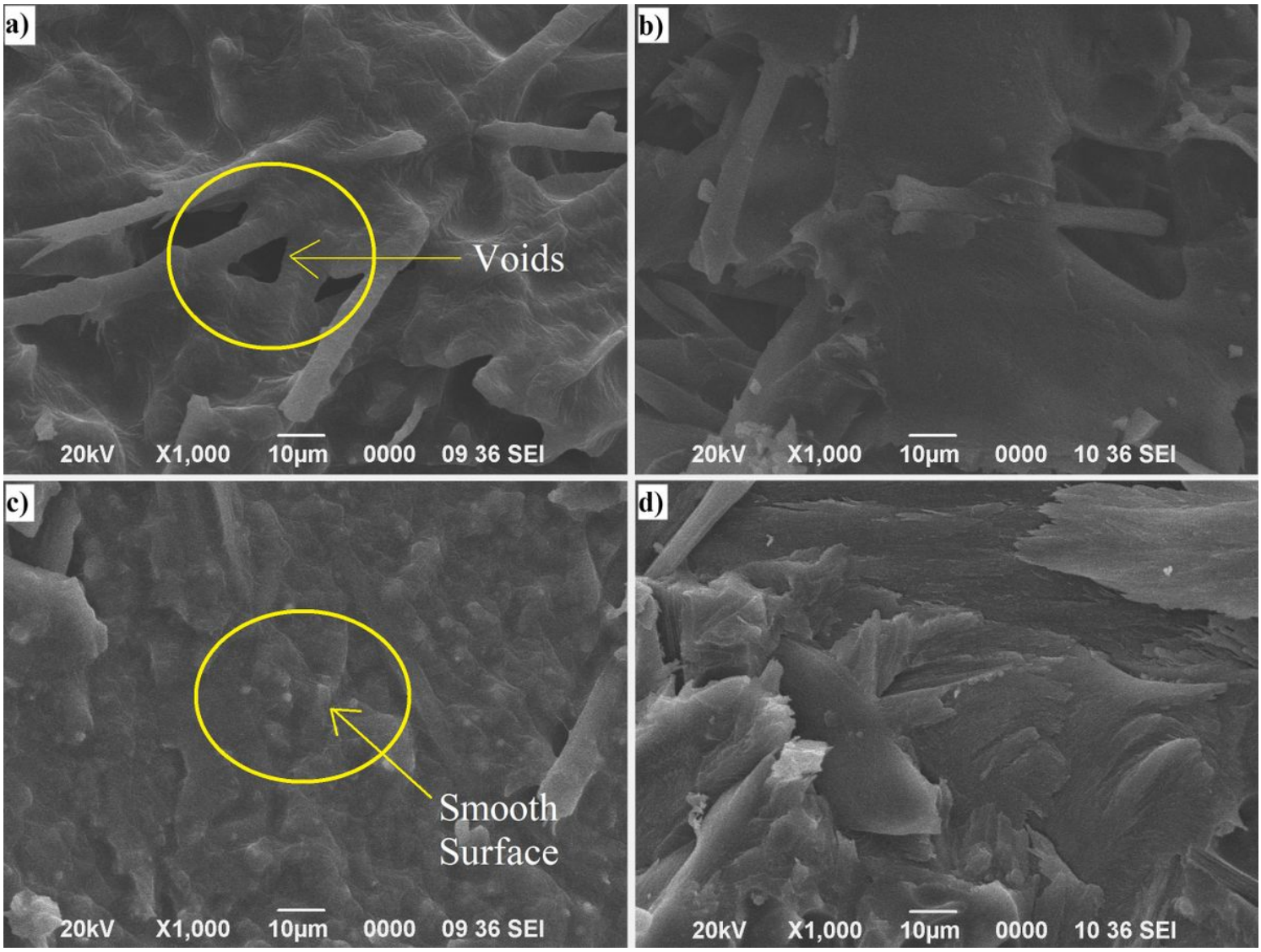

Figure 11

SEM micrographs of a) MAESO/CF/TM0 b) MAESO/CF/TM20 c) MAESO/CF/TM30 d) MAESO/CF/TM40

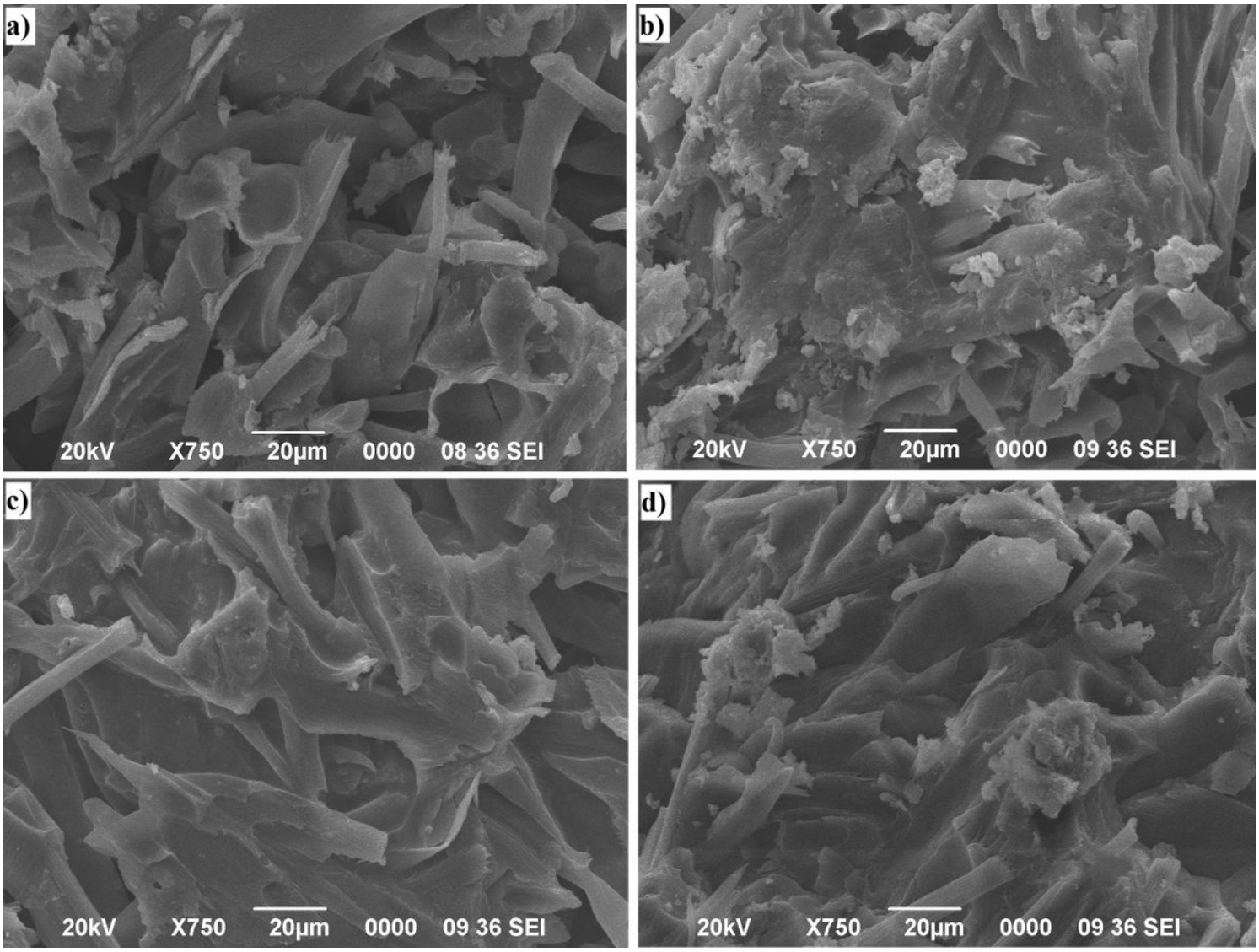

Figure 12

SEM micrographs of UV exposed samples a) MAESO/CF/TM0 b) MAESO/CF/TM20 c) MAESO/CF/TM30 d) MAESO/CF/TM40

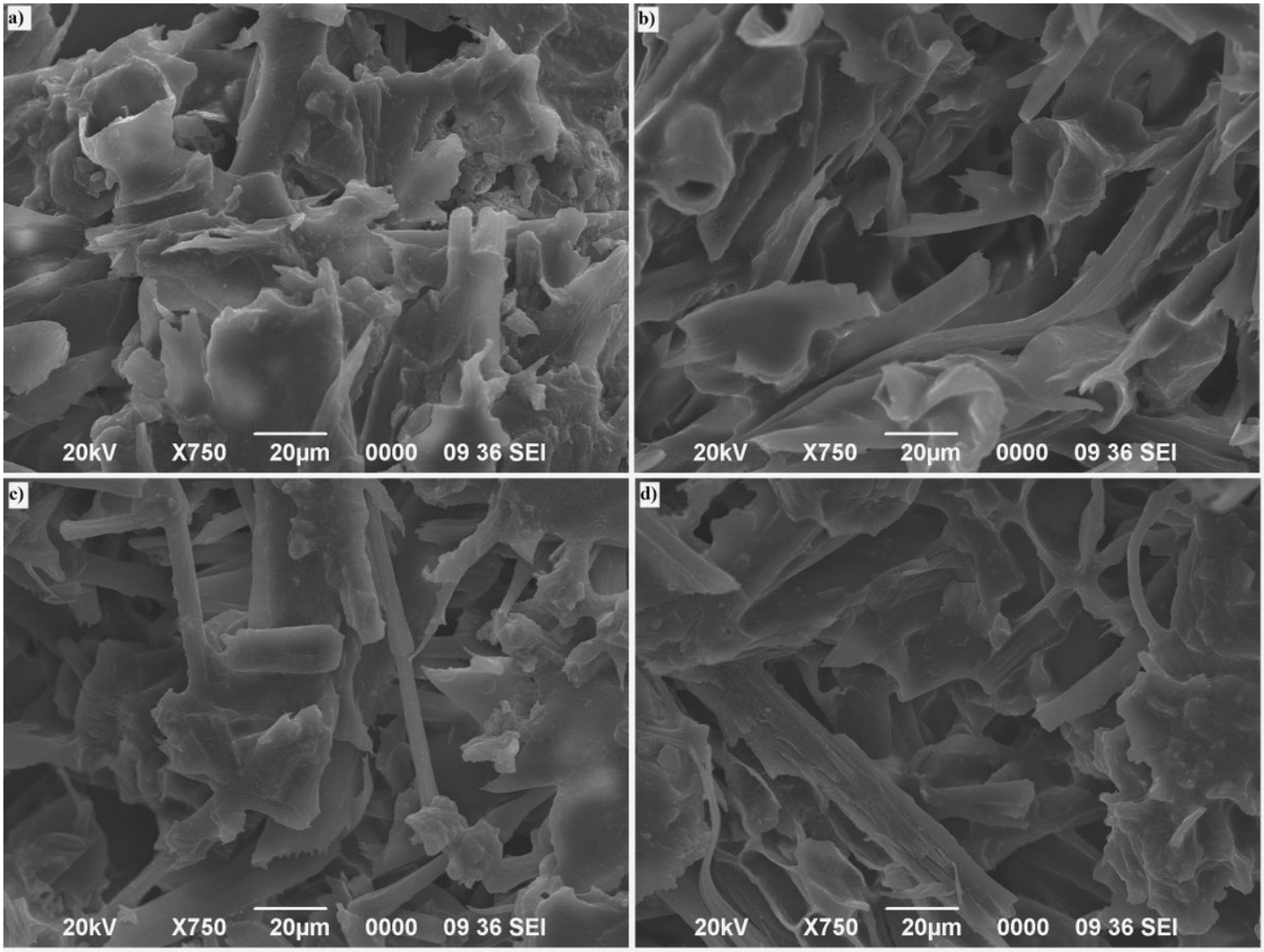

Figure 13

SEM micrographs of biodegraded samples a) MAESO/CF/TM0 b) MAESO/CF/TM20 c) MAESO/CF/TM30 d) MAESO/CF/TM40

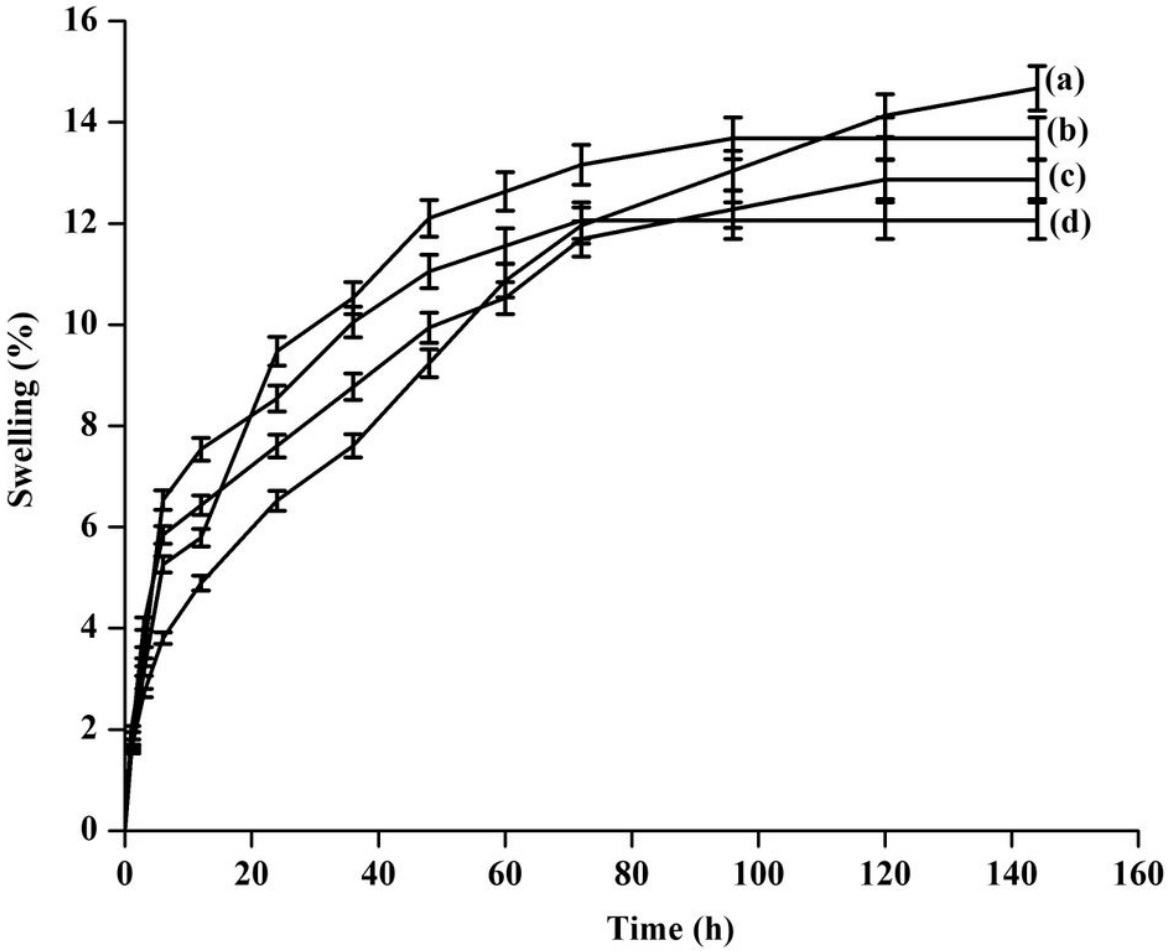

Figure 14

Water absorption of a) MAESO/CF/TM0 b) MAESO/CF/TM20 c) MAESO/CF/TM40 d) MAESO/CF/TM30

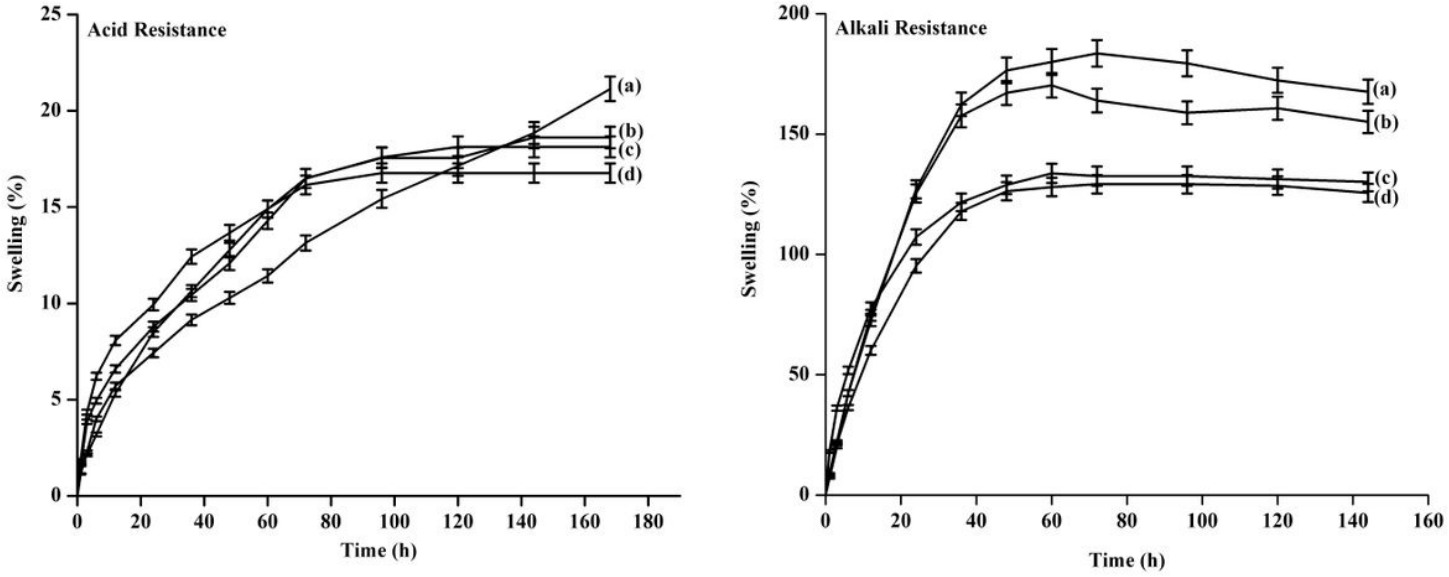

Figure 15

Chemical Resistance of a) MAESO/CF/TM0 b) MAESO/CF/TM20 c) MAESO/CF/TM40 d) MAESO/CF/TM30